

Autocrine IGF-1 Action in Adipocytes Controls Systemic IGF-1 Concentrations and Growth

Nora Klötting,¹ Linda Koch,² Thomas Wunderlich,² Matthias Kern,¹ Karen Ruschke,¹ Wilhelm Krone,³ Jens C. Brüning,² and Matthias Blüher^{1,3,4}

OBJECTIVE—IGF-1 and the IGF-1 receptor (IGF-1R) have been implicated in the regulation of adipocyte differentiation and lipid accumulation *in vitro*.

RESEARCH DESIGN AND METHODS—To investigate the role of IGF-1 receptor *in vivo*, we have inactivated the *Igf-1r* gene in adipose tissue (IGF-1R^{ap2Cre} mice) using conditional gene targeting strategies.

RESULTS—Conditional IGF-1R inactivation resulted in increased adipose tissue mass with a predominantly increased lipid accumulation in epigonadal fat pads. However, insulin-stimulated glucose uptake into adipocytes was unaffected by the deletion of the IGF-1R. Surprisingly, IGF-1R^{ap2Cre} mice exhibited markedly increased somatic growth in the presence of elevated IGF-1 serum concentrations, and IGF-1 mRNA expression was significantly increased in liver and adipose tissue. IGF-1 stimulation of wild-type adipocytes significantly decreased IGF-1 mRNA expression, whereas the opposite effect was observed in IGF-1R-deficient adipocytes.

CONCLUSIONS—IGF-1R signaling in adipocytes does not appear to be crucial for the development and differentiation of adipose tissue *in vivo*, but we identified a negative IGF-1R-mediated feedback mechanism of IGF-1 on its own gene expression in adipocytes, indicating an unexpected role for adipose tissue IGF-1 signaling in the regulation of IGF-1 serum concentrations in control of somatic growth. *Diabetes* 57:2074–2082, 2008

Insulin and the structurally related IGFs provide essential signals for the control of embryonic and postnatal development (1) through binding of their respective tyrosine kinase receptors. Conventional gene targeting strategies used to abrogate insulin receptor and IGF-1 receptor (IGF-1R) signaling reveal severe phenotypes of both insulin receptor- and IGF-1R-deficient mice. While inactivating the insulin receptor results in embryonic lethality (2), mice with a whole-body inactivation of the *Igf-1r* gene die shortly after birth (3), whereas

heterozygous *Igf-1r* knockout mice have increased longevity, most likely due to greater resistance to oxidative stress (4). These data point to a role of IGF-1R signaling in the regulation of lifespan. To discern the relevance of IGF-1R signaling in individual tissues, mice with tissue-specific inactivation of the IGF-1R have been created. Tissue-specific knockout of the *Igf-1r* gene in osteoblasts displayed significant defects in bone formation with low levels of osteoblastogenesis (5), revealing a function of the IGF system in formation and maintenance of bone tissue. Mice with simultaneous functional inactivation of both insulin and IGF-1Rs in skeletal muscle have a low muscle mass and display muscle hypoplasia (6), suggesting that IGF-1 is a vital regulator of muscle development. Conversely, muscle-specific overexpression of IGF-1R resulted in local myofiber hyperplasia (7). β -Cell-specific deletion of the IGF-1R did not alter islet development but led to hyperinsulinemia and glucose intolerance in β IGF-1RKO mice (8). This model suggests that tissue-specific alterations in the IGF-1 signaling might have secondary effects on the organism.

Until now, the role of IGF-1R signaling in white adipose tissue (WAT) has remained unclear. In 3T3-L1 adipocytes, IGF-1 is an essential regulator of differentiation (9), and it was recently shown that IGF-1 stimulates both cell growth and lipogenesis during differentiation of human mesenchymal stem cells into adipocytes *in vitro* (10). However, the physiological role of IGF-1R signaling in adipose tissue *in vivo* has not been systematically studied. To investigate the role of the IGF-1R in the development and metabolism of adipose tissue, we generated mice lacking the IGF-1R in adipose tissue (IGF-1R^{ap2Cre}) using a conditional gene targeting approach based on the Cre recombinase. Subsequently, we characterized the consequences of IGF-1R deletion in adipose tissue on morphological and metabolic parameters of IGF-1R^{ap2Cre} mice up to an age of 32 weeks.

RESEARCH DESIGN AND METHODS

Generation of IGF-1R^{ap2Cre} mice. IGF-1R^{lox/wt} mice were created by inserting loxP [locus of crossover (x) in bacteriophage P1] sites flanking exon 3 of the *Igf-1r* gene using conditional gene targeting strategies and maintained on a pure C57BL/6 genetic background. A targeting vector was constructed encompassing 4.5 kb of intron 2 of the murine *Igf-1r* gene, a loxP site, an FRT-flanked neomycin resistance gene, 600-bp fragment containing exon 3, a second loxP site, and 1.3 kb of intron 3. Cre-mediated recombination and subsequent excision of exon 3 of the IGF-1R results in a frame shift after 213 codons, with an appended sequence of 27 amino acids followed by a stop codon in exon 4. Gene targeting was performed in Bruce4 ES cells. For transfection, 1×10^7 ES cells were transfected with 40 μ g DNA. G418/Ganciclovir double-resistant colonies were picked ~9 days after transfection and expanded on 96-well tissue culture dishes. Genomic DNA was extracted from each clone and analyzed by Southern blot and PCR analysis. Recovery, microinjection, and transfer of 3.5 day postcoitum embryos were performed according to standard procedures. Chimeric animals (80–90% chimerism based on coat color) were bred with FlpE deleter on a C57BL/6 background. Genotyping was performed by PCR on DNA extracted from tail biopsies using

From the ¹Department of Medicine, University of Leipzig, Leipzig, Germany; the ²Department of Mouse Genetics and Metabolism, Institute for Genetics, University of Cologne and Center of Molecular Medicine Cologne, Cologne, Germany; the ³Department of Internal Medicine II, University of Cologne and Center of Molecular Medicine Cologne, Cologne, Germany; and the ⁴Interdisciplinary Center for Clinical Research (IZKF), Leipzig, Germany. Corresponding authors: Jens C. Brüning, jens.brueening@uni-koeln.de; Matthias Blüher, bluma@medizin.uni-leipzig.de.

Received 29 October 2007 and accepted 22 April 2008.

Published ahead of print at <http://diabetes.diabetesjournals.org> on 28 April 2008. DOI: 10.2337/db07-1538.

N.K. and L.K. contributed equally to this work.

© 2008 by the American Diabetes Association. Readers may use this article as long as the work is properly cited, the use is educational and not for profit, and the work is not altered. See <http://creativecommons.org/licenses/by-nc-nd/3.0/> for details.

The costs of publication of this article were defrayed in part by the payment of page charges. This article must therefore be hereby marked "advertisement" in accordance with 18 U.S.C. Section 1734 solely to indicate this fact.

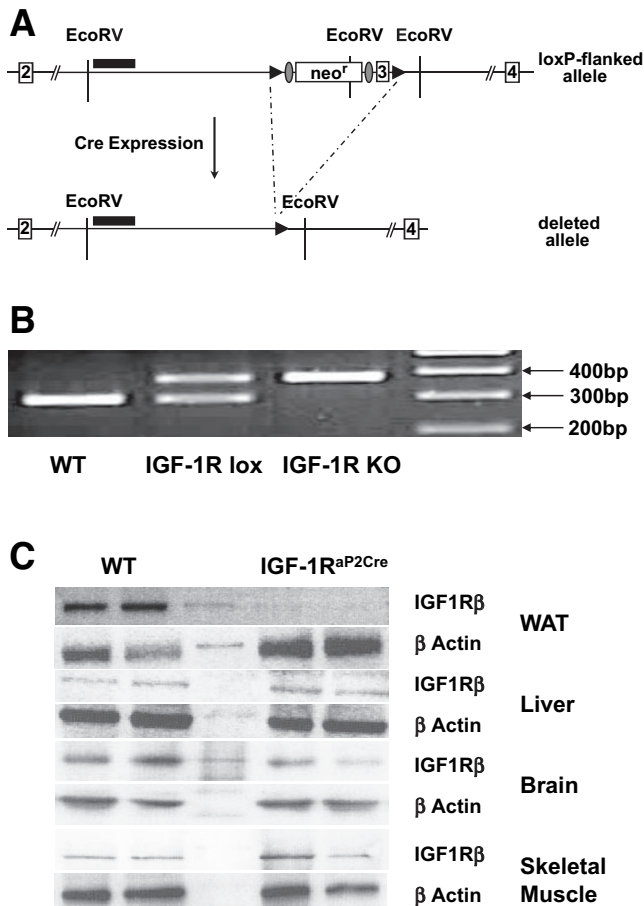


FIG. 1. Targeting strategy, assessment of IGF-1R recombination, and IGF-1R expression. **A:** Schematic representation of the loxP-flanked IGF-1R allele before and after recombination (Cre-expression). The knockout allele is shown below the floxed allele, indicating the deletion of exon 3 in the event of recombination of the *igf-1r* gene. BamHI, restriction sites; triangle, loxP site; ellipse, FRT site. **B:** Results from PCR analysis of DNA prepared from isolated adipocytes. DNA from isolated adipocytes of wild-type mice produced a 300-bp band (lane 1), whereas a single 380-bp band was detected for IGF-1R^{aP2Cre} mice (lane 3). Heterozygous expression of the transgene was detected by both a 300-bp and a 380-bp band (lane 2). **C:** Western blot analysis for IGF-1R β -subunit and β -actin as loading control of WAT, liver, brain, and skeletal muscle of two representative wild-type (WT) and IGF-1R^{aP2Cre} mice.

customized primers: 5'-TCC CTC AGG CTT CAT CCG CAA-3' (sense) and 5'-CTT CAG CTT TGC AGG TGC ACG-3' (antisense). The targeting strategy is shown in Fig. 1A. Mice on a mixed (C57BL/6 \times 129/Sv) genetic background carrying the *aP2* Cre transgene were made by cloning a 1.4-kb *SacI/SalI* complementary DNA fragment encoding the Cre recombinase, modified by inclusion of a nuclear localization sequence and a consensus polyadenylation signal, immediately downstream of the 5.4-kb promoter/enhancer of fatty acid-binding protein *aP2* (11).

IGF-1R^{aP2Cre} were derived by crossing IGF-1R^{lox/wt} mice with IGF-1R^{lox/wt} mice expressing the Cre recombinase under the control of the *aP2* promoter/enhancer (IGF-1Rhet^{aP2Cre}). All mice were housed in pathogen-free facilities in groups of three to five at 22 \pm 2°C on a 12-h light/dark cycle. Animals were fed a standard chow diet (Altromin, Lage, Germany). In a subgroup of six to eight female IGF-1R^{aP2Cre} and six wild-type mice, a high-fat diet study was performed with a special high-fat diet containing 55.2% of calories from fat (C1057; Altromin). Animals had ad libitum access to water at all times, and food was only withdrawn if required for an experiment. All experiments were performed in accordance with the rules for animal care of the local government authorities (Bezirksregierung Köln, Cologne, Germany) of the German Government and were approved by the institutional animal care and use committee.

Molecular characterization and genotyping of the IGF-1R^{aP2Cre} mice. Genotyping was performed by PCR using genomic DNA isolated from the tail tip. In brief, genomic DNA was prepared by using the DNeasy kit (Qiagen,

Hilden, Germany). The following two primer pairs were used to genotype *Igf-1r* loxP sites, 5'-TCC CTC AGG CTT CAT CCG CAA-3' (forward) and 5'-CTT CAG CTT TGC AGG TGC ACG-3' (reverse), as well as the *aP2* Cre recombinase 5'-CGC CGC ATA ACC AGT GAA AC-3' (forward) and 5'-ATG TCC AAT TTA CTG ACC G-3' (reverse). PCR was performed for 25 cycles (*loxP* sites) or 30 cycles (*aP2* Cre) of 95°C, 59°C (*loxP* sites), or 58°C (*aP2* Cre), and 72°C (30 s each) using the Qiagen *Taq* Polymerase and a Peltier Thermal Cycler PTC-200 (Bio-Rad, Hercules, CA). DNA from wild-type mice produced a 300-bp band, and a 380-bp band was detected in IGF-1R lox mice (Fig. 1B). For Western blot analysis, tissues were removed and homogenized in homogenization buffer with an ultra-Turrax homogenizer (IKA Werke, Stauffen, Germany), proteins were isolated using standard techniques, and Western blot analysis was performed with antibodies raised against IGF-1R β -subunit (Santa Cruz Biotechnology, C20) and β -actin (Abcam, Cambridge, U.K.) as loading control.

Phenotypic characterization. Ten mice of each genotype (IGF-1R^{aP2Cre}, IGF-1Rhet^{aP2Cre}, wild-type, IGF-1R^{lox/lox}, and *aP2* Cre) of both sexes were studied from an age of 4 weeks up to 32 weeks of life. Body weight was recorded weekly up to an age of 14 weeks, and thereafter in 2-week intervals; body length (naso-anal length) was measured once at week 32. At an age of 16 weeks, both sexes of a subgroup of 20 (10 IGF-1R^{aP2Cre} and 10 controls) underwent a food intake measurement over a time period of 1 week. The daily food intake was calculated as the average intake of chow within the time stated. Intraperitoneal glucose tolerance tests (GTTs) and insulin tolerance tests (ITTs) were performed at the age of 12 and 24 weeks. GTT was performed after an overnight fast for 16 h by injecting 2 g/kg body wt glucose and measuring the blood glucose levels after tail vein incision at 0 (baseline), 10, 30, 60, and 120 min after injection. ITT was performed in random-fed animals by injecting 0.75 unit/kg body wt human regular insulin (40 units Actrapid; Novo Nordisk, Copenhagen, Denmark). Glucose levels were determined in blood collected from the tail tip immediately before and 15, 30, and 60 min after the intraperitoneal injection.

Mice were killed at the age of 32 weeks by an overdose of anesthetic (Sevofluran, Abbott, Germany). Liver, heart, brain, lung, spleen, subcutaneous, and epigonadal adipose tissue were immediately removed. The organs were weighed and related to the whole-body mass to obtain relative organ weights. Serum was collected at 32 weeks, and concentrations of insulin, leptin, adiponectin, and IGF-1 were measured.

Analytical procedures. Blood glucose values were determined from whole-venous blood samples using an automated glucose monitor (GlucoMen; Menarini Diagnostics, Wokingham, U.K.). Insulin, leptin, growth hormone (GH), and adiponectin serum concentrations were measured by ELISA using mouse standards according to the manufacturer's guidelines (Mouse/Rat Insulin ELISA; Linco, St. Charles, MO) (Mouse Leptin ELISA and Mouse Adiponectin/Acrp30 ELISA; R&D Systems, Minneapolis, MN). IGF-1 serum concentrations were measured by a radioimmunoassay (Mediagnost, Reutlingen, Germany).

Adipocyte isolation, size distribution, and primary culture. Animals were killed, and subcutaneous and epididymal fat pads were removed. Adipocytes were isolated by 1 mg/ml collagenase digestion. To determine cell size distribution and adipocyte number, 200- μ l aliquots of adipocytes were fixed with osmic acid, incubated for 48 h at 37°C, and counted in a Coulter counter (Multisizer III; Beckman Coulter, Krefeld, Germany). Isolated adipocytes were resuspended in Dulbecco's modified Eagle's medium/F-12 Ham's medium (Sigma, St. Louis, MO) and centrifuged at 350 \times g for 10 min to separate mature adipocytes from the stromal vascular cell pellet, which was discarded. Floating fat-filled adipocytes were then incubated for 6 h with different concentrations (0, 0.1, 1, 10, and 100 ng/ml recombinant IGF-1 (U.S. Biological, Swampscott, MA)).

Histology. Tissue was fixed in 4% buffered formaldehyde, trimmed into small cubes, rinsed in phosphate-buffered saline, and dehydrated in a graded series of 50–100% ethanol followed by propylene oxide. Tissue was infiltrated with propylene:epon 812 mixtures by increasing the resin concentration gradually. Sections at 0.5 μ m were cut with a Reichert ultramicrotome, mounted on polylysine-covered object slides and stained with azur-II-methylene blue (Richardson stain). Digitized pictures were taken with the light microscope Axioplan 2 (Zeiss, Jena, Germany) using the measurement facilities of Imagic Access (Imagic, Glattburg, Switzerland). Multiple sections (separated by 70–80 μ m each) were obtained from gonadal and subcutaneous fat pads and analyzed systematically with respect to adipocyte size and number. For each genotype and sex, at least 10 fields (representing \sim 100 adipocytes) per slide were analyzed.

Glucose transport. For the determination of glucose transport, isolated adipocytes from the different fat depots were stimulated with 100 nmol/l insulin for 30 min and then incubated for 30 min with 3 μ mol/l [14 C]glucose. Immediately after incubation, adipocytes were fixed with osmic acid and

incubated for 48 h at 37°C, and radioactivity was quantified after the cells had been decolorized (12).

Tissue-specific IGF-1 mRNA expression. IGF-1 mRNA expression was measured by quantitative real-time PCR using the standard curve method in a fluorescent temperature cycler using the TaqMan assay. Fluorescence was detected on an ABI PRISM 7000 sequence detector (Applied Biosystems, Darmstadt, Germany). Total RNA was extracted from epigonadal and subcutaneous WAT, primary adipocyte culture after incubation with or without IGF-1, liver, brain, skeletal muscle, and brown adipose tissue (BAT) using TRIzol (Life Technologies, Grand Island, NY), and 1 µg RNA was reverse transcribed with standard reagents (Life Technologies, Grand Island, NY). From each RT-PCR, 2 µl was amplified in a 26-µl PCR using the Brilliant SYBR Green QPCR Core Reagent kit from Stratagene (La Jolla, CA) according to manufacturer's instructions. The following primer pairs were used: muIGF-1, 5'-GCTGCTGAAGCCATTCATTT-3' (sense) and 5'-TTGCTCTTAAGGAGGC-CAAA-3' (antisense); mu36B4, 5'-aacatgctcaacatctcccc-3' (sense) and 5'-ccgactctccgactcttc-3' (antisense). Expression of IGF-1 and 36B4 mRNA were quantified by using the second derivative maximum method of the TaqMan software (Applied Biosystems) determining the crossing points of individual samples by an algorithm that identifies the first turning point of the fluorescence curve. Amplification of specific transcripts was confirmed by melting curve profiles (cooling the sample to 68°C and heating slowly to 95°C with measurement of fluorescence) at the end of each PCR.

Data analysis and statistics. Data are given as means ± SD. Datasets were analyzed for statistical significance using a two-tailed unpaired Student's *t* test, or differences were assessed by one-way ANOVA corrected by Bonferroni-Holm using the Statistical Package for Social Science, version 14.0 (SPSS, Chicago, IL). *P* values <0.05 were considered significant.

RESULTS

Generation of IGF-1R^{aP2Cre} mice. Mice lacking the IGF-1R in adipose tissue (IGF-1R^{aP2Cre}) were generated by crossing mice carrying the loxP-flanked *Igf-1r* allele with transgenic mice expressing the Cre recombinase under control of the adipose-specific fatty acid binding protein (*aP2*) promoter. The targeting strategy is shown in Fig. 1A. IGF-1R^{aP2Cre} mice were obtained with the expected Mendelian frequency. Cre expression was expected to be restricted to WAT and BAT. PCR analysis of the genomic DNA showed that the wild-type *Igf-1r* allele was absent in IGF-1R^{aP2Cre}, whereas IGF-1Rhet^{aP2Cre} mice contained both the wild-type and loxP-flanked *Igf-1r* allele (Fig. 1B). Western blot analysis of adipose tissue lysates clearly indicated that *Igf-1r* protein was reduced by ~90% in WAT of IGF-1R^{aP2Cre} mice (Fig. 1C) and completely lost in BAT (data not shown). A ~40% reduction of IGF-1R protein expression was found in the brain, whereas no changes in the overall expression of the IGF-1R protein were detected in liver, skeletal muscle (Fig. 1C), kidney, and bone (data not shown). IGF-1R expression was unaffected in all tissues of wild-type, IGF-1R^{lox/lox}, and aP2 Cre mice, indicating that neither the loxP modification of the IGF-1R locus nor expression of the aP2 transgene alone affects IGF-1R expression. These genotypes (wild type, IGF-1R^{lox/lox}, and aP2 Cre) had similar physiological and metabolic characteristics and were therefore considered controls in all subsequent analyses.

Phenotype of IGF-1R^{aP2Cre} mice. Both sexes of IGF-1R^{aP2Cre} mice exhibited normal growth until the age of 10 weeks. However, by 10 weeks of age male and female IGF-1R^{aP2Cre} mice had gained more weight than control group littermates (Fig. 2A and B). Moreover, we found that IGF-1R^{aP2Cre} mice had significantly increased naso-anal body length when compared with littermate controls (females, *P* < 0.01; and males, *P* < 0.001) at an age of 24 and 32 weeks (Fig. 2C). Heterozygous deficiency of the *Igf-1r* gene had no significant influence on body growth and weight (data not shown). Daily food intake was indistinguishable between IGF-1R^{aP2Cre} mice and all control groups (data not shown). Because IGF-1R^{aP2Cre} mice ex-

hibit ~15% increased body weight, organ and fat pad weights were calculated as percentage of the whole-body weight at an age of 24 weeks. We found a disproportional increase of fat pad (Fig. 2D), liver (Fig. 2E), and heart weights in IGF-1R^{aP2Cre} mice. In contrast, relative brain weight was significantly reduced in IGF-1R^{aP2Cre} compared with controls (Fig. 2F). Relative organ weights of BAT (Fig. 2G), skeletal muscle, kidney, spleen, and bone were not different between IGF-1R^{aP2Cre} mice and control mice (data not shown).

Metabolic parameters. To determine the physiological consequences of reduced adipose tissue IGF-1R expression, we monitored blood glucose, insulin, total cholesterol, and triglyceride concentrations and performed serial glucose and ITTs over an age range from 12 to 32 weeks (Table 1). Fasted blood glucose was significantly higher in IGF-1R^{aP2Cre} mice at an age of 12 weeks, whereas no such differences were found at 24 weeks of age (Table 1). In parallel, fed blood glucose was significantly higher at an age of 12 weeks in males (Table 1). There were no differences in serum insulin and leptin concentrations between IGF-1R^{aP2Cre} and control mice at 12 and 24 weeks (Table 1). Cholesterol and triglyceride serum concentrations were also not significantly different between IGF-1R^{aP2Cre} and control mice (Table 1). Adiponectin serum concentrations were higher in control compared with IGF-1R^{aP2Cre} mice, however, these differences were only significant at 12 weeks (Table 1). Independent of age, intraperitoneal GTTs demonstrated normal glucose tolerance in male (Fig. 3A and B) and female (data not shown) IGF-1R^{aP2Cre} and control mice. Intraperitoneal ITTs at 12 and 24 weeks of age in male (Fig. 3C and D) and female mice (data not shown) were indistinguishable between IGF-1R^{aP2Cre} and control mice. Taken together, reducing IGF-1R expression in adipose tissue results in increased somatic growth in the absence of major metabolic alterations.

IGF-1 serum concentration is markedly increased in IGF-1R^{aP2Cre} mice. Because IGF-1R^{aP2Cre} mice exhibited an increased postnatal somatic growth, we next determined circulating plasma IGF-1 concentrations as the major determinant of somatic growth in mammals. IGF-1 serum concentration is significantly increased in IGF-1R^{aP2Cre} mice starting at an age of 12 weeks up to 24 weeks of age (Fig. 4A). In parallel to higher IGF-1 serum concentrations, we found significantly higher serum concentrations of the IGF binding protein (IGFBP)-3 (Fig. 4B). On the other hand, serum concentrations of IGFBP-1 and -2 were not significantly different between IGF-1R^{aP2Cre} and control mice (data not shown). GH and IGF-2 serum concentrations were indistinguishable between IGF-1R^{aP2Cre} and control mice (Table 1), indicating that dysregulation of IGF-1 concentrations is not a result of altered pituitary regulation and thus appears to be primarily regulated in peripheral organs of IGF-1R^{aP2Cre} mice. Therefore, we determined IGF-1 and IGFBP-3 mRNA expression in adipose tissue and liver of IGF-1R^{aP2Cre} and control mice to assess whether increased IGF-1 and IGFBP-3 serum concentrations correlate with increased expression in those organs important for the synthesis of these molecules. We found significantly higher IGF-1 mRNA expression both in adipose tissue (Fig. 4C) and liver (Fig. 4D) of IGF-1R^{aP2Cre} mice. In parallel, there was a trend for increased IGFBP-3 mRNA expression in liver and adipose tissue of IGF-1R^{aP2Cre} compared with control mice (data not shown).

To determine whether increased adipose tissue IGF-1

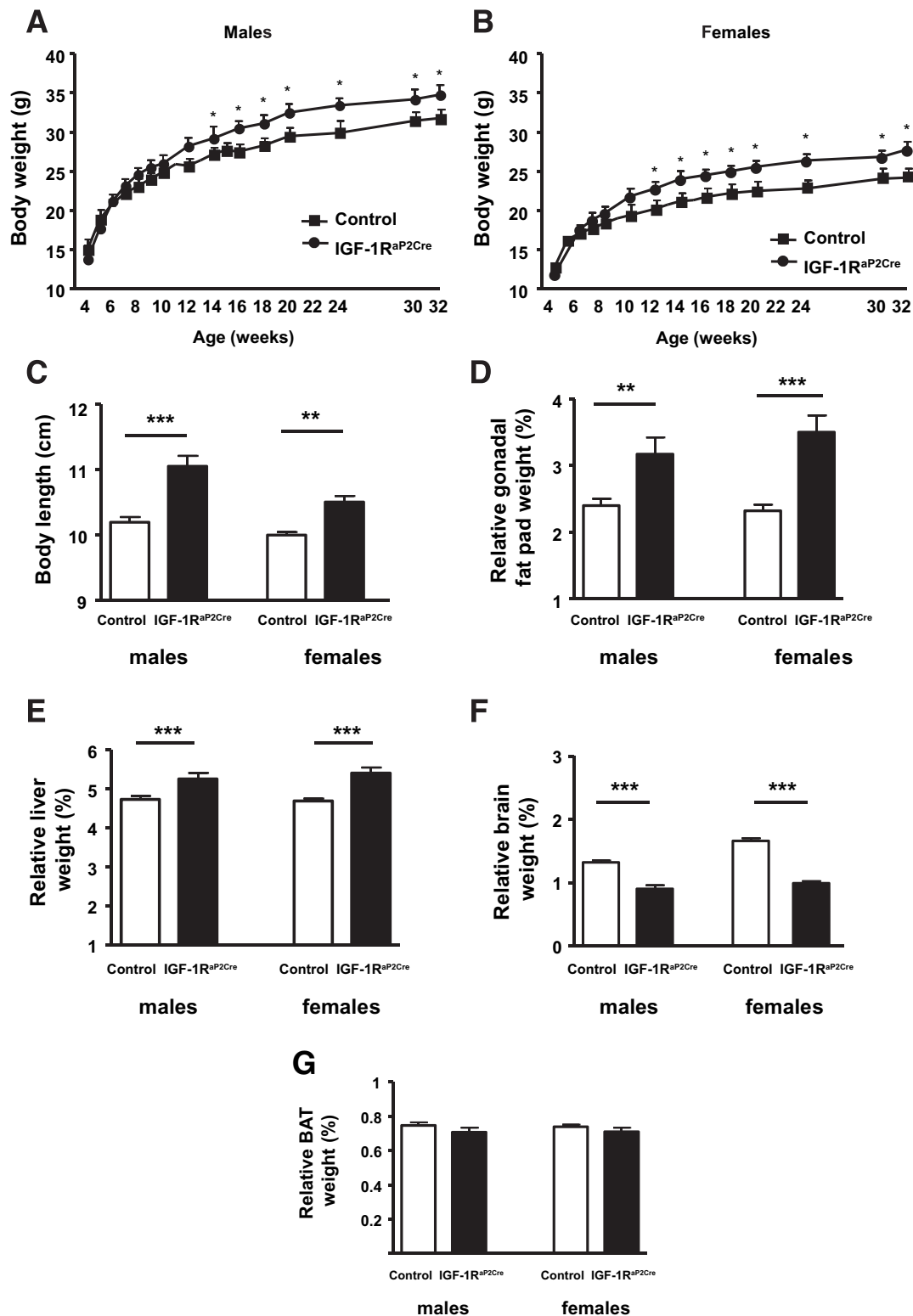


FIG. 2. Growth phenotype of IGF-1R^{aP2Cre} mice and controls. IGF-1R^{aP2Cre} mice show identical growth until an age of 10 weeks. Thereafter, body weight of IGF-1R^{aP2Cre} mice is significantly increased both in males (A) and females (B) until an age of 32 weeks. * $P < 0.05$, ** $P < 0.01$, *** $P < 0.001$. C: Body length (naso-anal length) is markedly increased in IGF-1R^{aP2Cre} mice at an age of 24 weeks ($n = 10$ per genotype and sex). D–F: Organ weights relative to body weight in 24-week-old IGF-1R^{aP2Cre} and control mice ($n = 10$ per genotype and sex). IGF-1R^{aP2Cre} mice exhibit increased relative epigonadal fat pad (D) and liver weight (E). Relative brain weight (F) was significantly reduced in IGF-1R^{aP2Cre} mice, possibly as a consequence of heterozygous transgene (aP2) expression in brain, whereas relative BAT weight (G) was indistinguishable between IGF-1R^{aP2Cre} and control mice.

expression in IGF-1R^{aP2Cre} mice was the result of an altered adipocyte autonomous autocrine regulatory loop, we isolated adipocytes from wild-type and IGF-1R^{aP2Cre}

mice. Treatment of control adipocytes with recombinant IGF-1 (100 ng/ml) for 6 h ex vivo caused a significant reduction of its own mRNA expression (Fig. 4E). Con-

TABLE 1
Metabolic parameters in 12- and 24-week-old male and female IGF-1R^{aP2Cre} and control mice

	Age (weeks)	Males		Females	
		Control	IGF-1R ^{aP2Cre}	Control	IGF-1R ^{aP2Cre}
<i>n</i>		10	10	10	10
Blood glucose, fasted (mg/dl)	12	82 ± 18*	111 ± 35	74 ± 17†	99 ± 20
	24	91 ± 22	106 ± 33	88 ± 18	91 ± 20
Blood glucose, fed (mg/dl)	12	149 ± 16†	169 ± 15	141 ± 18	147 ± 16
	24	144 ± 17	153 ± 12	137 ± 15	140 ± 15
Serum insulin, fasted (ng/ml)	24	1.8 ± 1.5	1.5 ± 0.5	0.4 ± 0.2	0.6 ± 0.4
Serum leptin, fed (pg/ml)	24	10.1 ± 4.8	8.2 ± 4.8	10.6 ± 5.4	12.1 ± 5.2
Growth hormone, fed (ng/ml)	24	11.4 ± 5.2	10.8 ± 6.1	9.5 ± 4.7	10.2 ± 5.8
IGF-2, fed (μg/ml)	24	1.13 ± 0.5	1.08 ± 0.4	0.97 ± 0.6	1.11 ± 0.6
Serum adiponectin, fed (ng/ml)	12	7.5 ± 1.6‡	4.7 ± 0.8	16.1 ± 1.2‡	8.9 ± 2.2
	24	9.5 ± 4.1	6.4 ± 1.9	16.5 ± 6.8	12.5 ± 7.7
Serum cholesterol, fed (mmol/l)	24	2.5 ± 0.5	2.4 ± 0.5	1.9 ± 0.3	2.1 ± 0.2
Serum triglycerides, fed (mmol/l)	24	1.7 ± 0.7	1.5 ± 0.9	1.1 ± 0.1	1.8 ± 1.2

Significant differences from control: **P* < 0.05, †*P* < 0.01, ‡*P* < 0.001.

versely, in adipocytes from IGF-1R^{aP2Cre} mice, stimulation with IGF-1 did not inhibit *IGF-1* mRNA expression but rather resulted in a paradoxical stimulation of IGF-1 mRNA expression.

Consequences of IGF-1R knockout on adipose tissue morphology and metabolism. Adipose tissue mass is increased in IGF-1R^{aP2Cre} mice compared with controls (Fig. 2D). The increased adipose tissue mass was related

to both increased number and mean volume of adipocytes in IGF-1R^{aP2Cre} mice (data not shown). Mean adipocyte size (diameter) is significantly higher in IGF-1R^{aP2Cre} (105.4 ± 12 μm) when compared with control (87.3 ± 9.3 μm) mice (*P* < 0.05). These differences are more pronounced in epigonadal than in subcutaneous fat (Fig. 5A and B). We found a 1.4-fold increase in insulin receptor mRNA expression in adipocytes from IGF-1R^{aP2Cre} mice

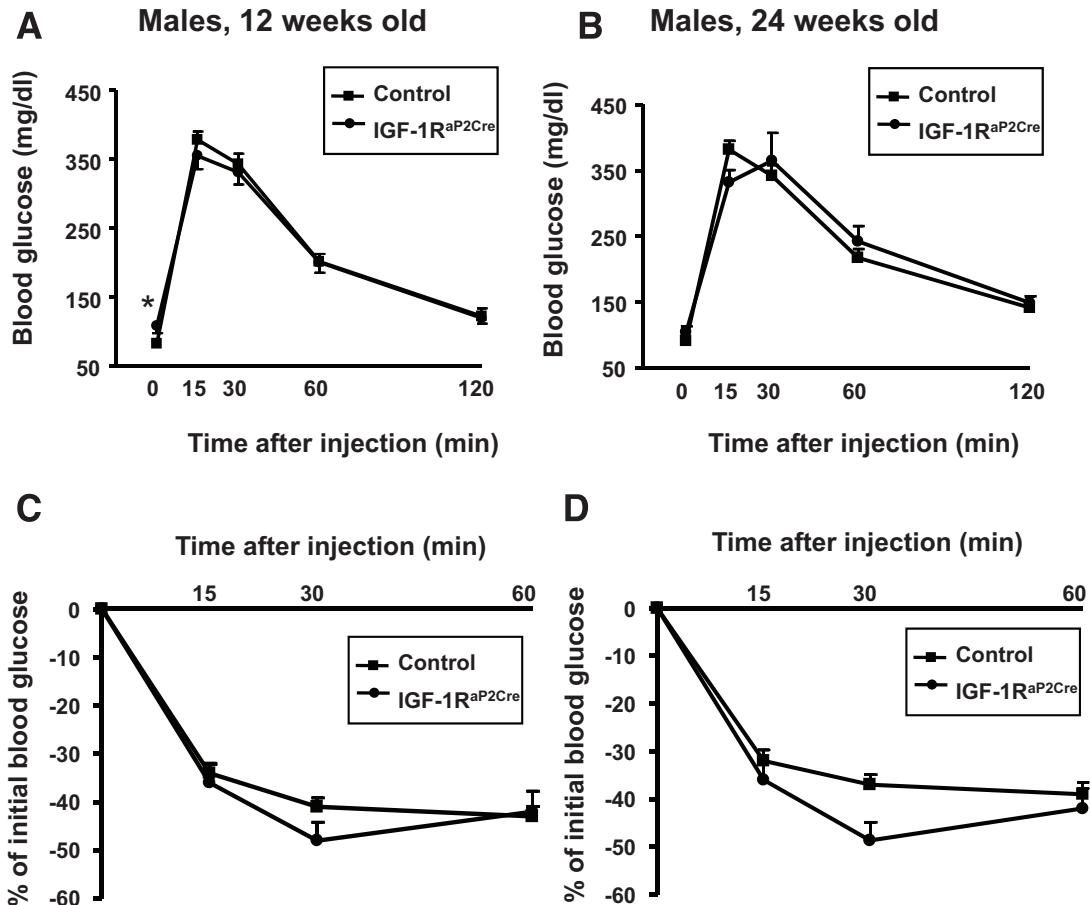


FIG. 3. IGF-1R^{aP2Cre} mice have normal glucose tolerance and insulin sensitivity. A and B: GTTs performed on 12-h-fasted 12-week old (A) and 24-week-old (B) male wild-type (control) and IGF-1R^{aP2Cre} mice. Results are expressed as means ± SE from 10 animals per genotype. C and D: ITTs on random fed 12-week-old (C) and 24-week-old (D) male wild-type (control) and IGF-1R^{aP2Cre} mice. Results are expressed as means ± SE from 10 animals per genotype.

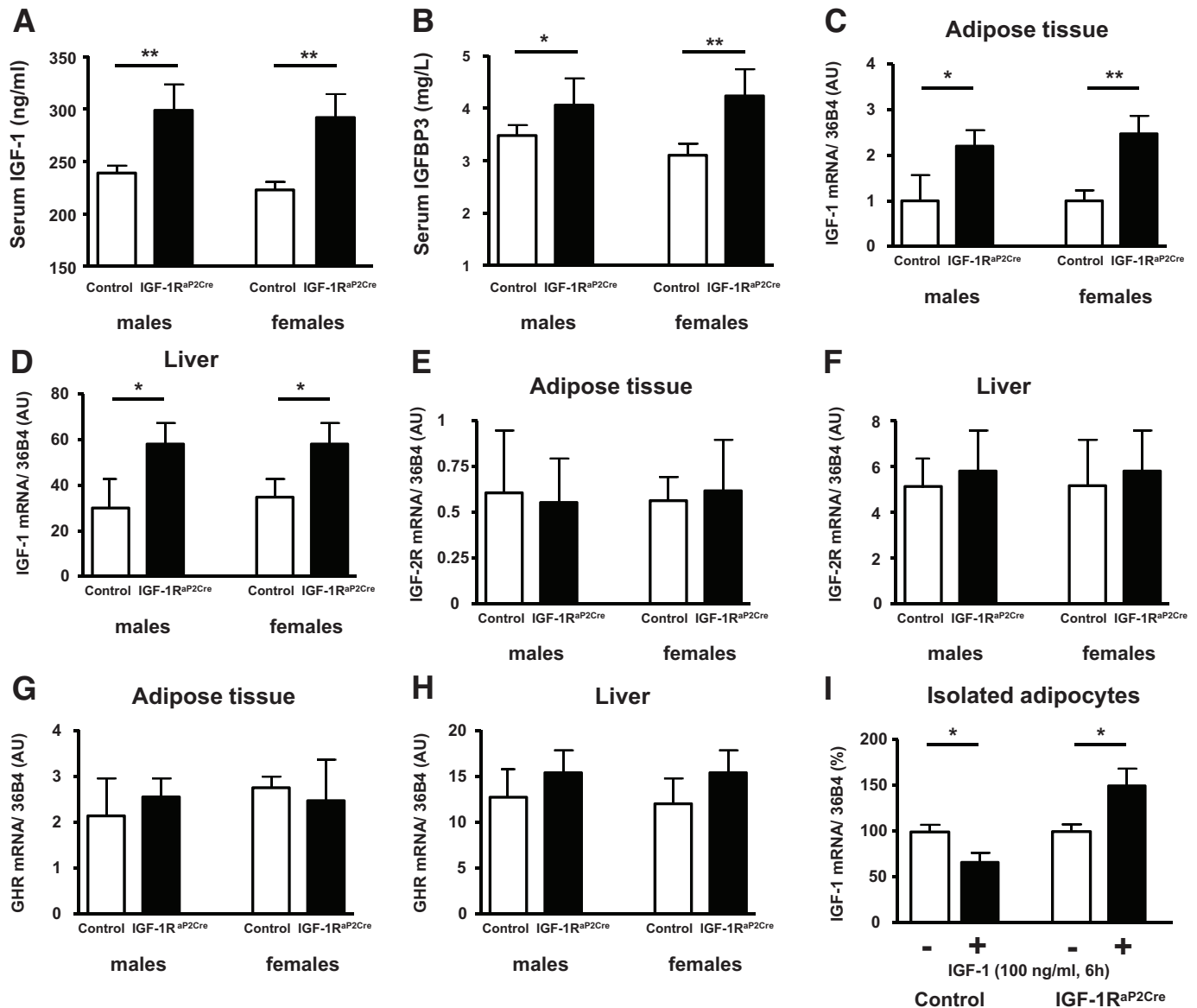


FIG. 4. IGF-1, IGF-1R, and IGF-1 mRNA expression in adipose tissue and liver of IGF-1R^{aP2Cre} and wild-type (control) mice. **A:** IGF-1 serum concentrations are significantly higher in IGF-1R^{aP2Cre} compared with wild-type mice. ** $P < 0.01$, $n = 10$ per genotype and sex. **B:** Higher IGF-1R^{aP2Cre} serum concentrations in IGF-1R^{aP2Cre} compared with wild-type mice. * $P < 0.05$, $n = 5$ per genotype and sex. **C and D:** IGF-1 mRNA expression in adipose tissue (**C**) and liver (**D**). * $P < 0.05$, ** $P < 0.01$; $n = 10$ per genotype and sex. **E and F:** IGF-2R mRNA expression in adipose tissue (**E**) and liver (**F**). **G and H:** GH receptor (GHR) mRNA expression in adipose tissue (**G**) and liver (**H**). **I:** IGF-1 mRNA expression in isolated adipocytes from 24-week-old male ($n = 5$ per genotype) after 6 h of incubation with or without 100 ng/ml recombinant murine IGF-1. * $P < 0.05$. Values are means \pm SE. AU, arbitrary units. *Igf-1* mRNA expression was calculated relative to the mRNA expression of *36B4*.

(data not shown). To determine the consequences of IGF-1R knockout on adipocyte glucose transport, basal and insulin-stimulated glucose uptake in isolated adipocytes was studied. In adipocytes from IGF-1R^{aP2Cre} mice, basal glucose uptake is unchanged compared with wild-type mice (Fig. 5C). Insulin stimulated glucose uptake is 2.8-fold in IGF-1R^{aP2Cre} and 2.1-fold in wild-type adipocytes ($P < 0.05$). Despite larger adipocyte size in IGF-1R^{aP2Cre} mice, we found significantly increased insulin sensitivity in IGF-1R^{aP2Cre} compared with wild-type adipocytes.

DISCUSSION

IGFs (IGF-1 and -2) lead to many different biological effects in target cells such as hepatocytes, myocytes, and adipocytes (13). IGF-1 action is propagated by the IGF-1R. IGF-1R-deficient mice are severely growth retarded, exhibit multiple growth- and differentiation-dependent abnormalities, and die

shortly after birth (3). Disruption of IGF-1R in specific tissues or cell types such as osteoblasts (5), skeletal muscle (6), and β -cells (8) further revealed an essential role of IGF-1R signaling in differentiation and growth.

IGF-1 was shown to be an essential regulator of differentiation in 3T3L1 adipocytes (9). Moreover, IGF-1 stimulates both cell growth and lipogenesis during differentiation of human mesenchymal stem cells into adipocytes in vitro (10). However, the physiological role of the IGF-1R signaling in adipose tissue in vivo has not been systematically studied. We therefore created mice lacking the IGF-1R in adipose tissue (IGF-1R^{aP2Cre} mice). To specifically target adipose tissue, we used transgenic mice that express the Cre recombinase cDNA from the adipose-specific fatty acid binding protein (aP2) promoter/enhancer (14). aP2 Cre mice have been used for adipose-selective inactivation

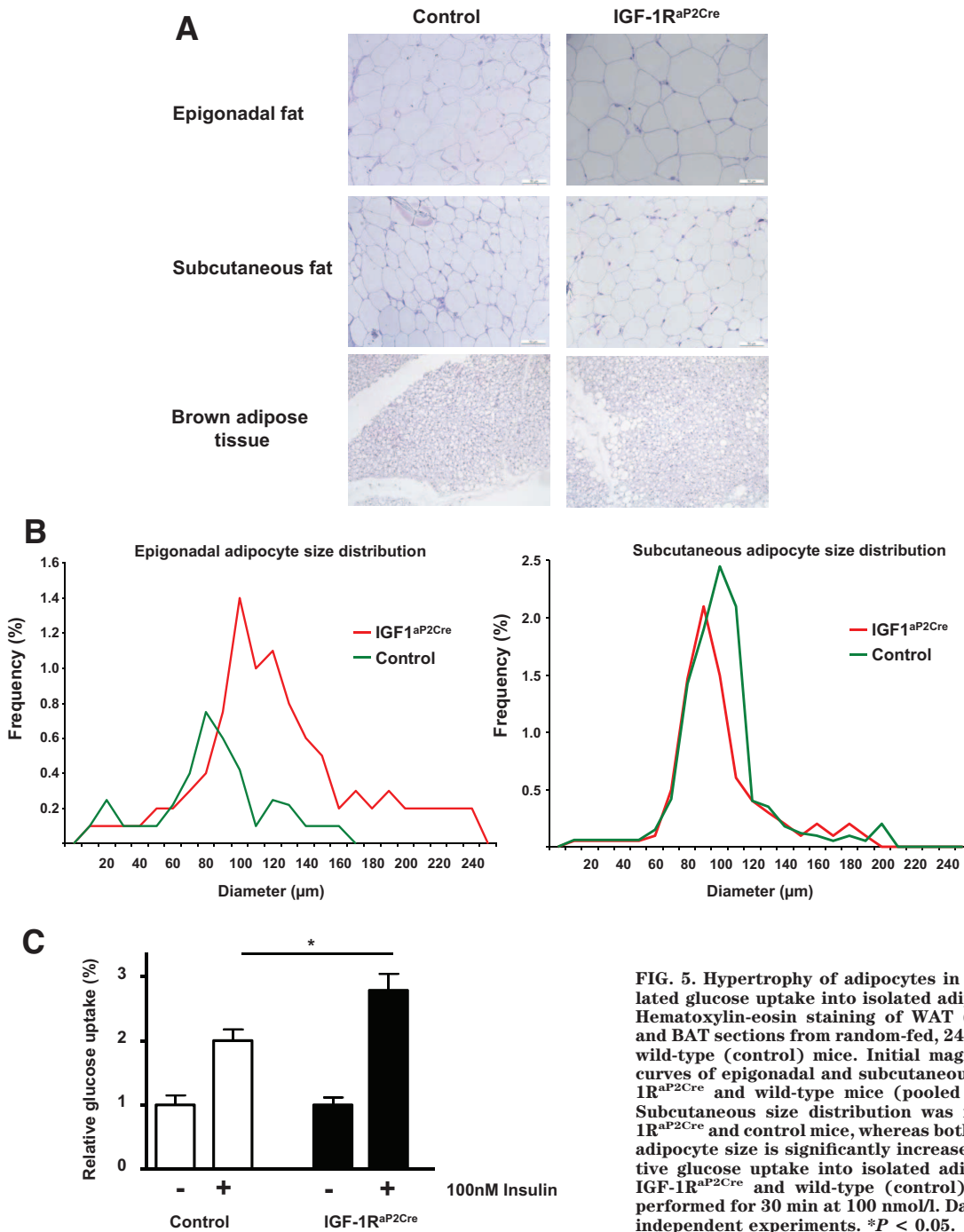


FIG. 5. Hypertrophy of adipocytes in WAT and normal insulin stimulated glucose uptake into isolated adipocytes of IGF-1R^{aP2Cre} mice. **A:** Hematoxylin-eosin staining of WAT (epigonadal and subcutaneous) and BAT sections from random-fed, 24-week-old male IGF-1R^{aP2Cre} and wild-type (control) mice. Initial magnification, ×10. **B:** Distribution curves of epigonadal and subcutaneous isolated adipocytes from IGF-1R^{aP2Cre} and wild-type mice (pooled from five mice per genotype). Subcutaneous size distribution was indistinguishable between IGF-1R^{aP2Cre} and control mice, whereas both mean and maximum epigonadal adipocyte size is significantly increased in IGF-1R^{aP2Cre} mice. **C:** Relative glucose uptake into isolated adipocytes from 24-week-old male IGF-1R^{aP2Cre} and wild-type (control) mice. Insulin stimulation was performed for 30 min at 100 nmol/l. Data represent means ± SE of five independent experiments. **P* < 0.05.

of the *GLUT4* and *insulin receptor* genes (11,15,16). Unexpectedly, deletion of IGF-1R was not restricted to WAT and BAT. In most IGF-1R^{aP2Cre} mice, we found a reduction of IGF-1R protein also in the brain, suggesting transgene expression in neuronal tissue in addition to fat. Although aP2 promoter provides adipocyte-restricted expression postnatally, it was recently shown that aP2 has a wider embryonic expression pattern than previously appreciated (17). Throughout embryonic development, the aP2 Cre transgene was consistently found in different cell types of the nervous system (17). Expression of the aP2 Cre transgene during embryonic development might explain the reduced relative brain mass in IGF-1R^{aP2Cre} mice. We excluded aP2 Cre transgene expression in other tissues, including liver and skeletal muscle, by protein ex-

pression analyses. Whole-body expression of the transgene would cause growth retardation as demonstrated in *IGF-1r*^{+/-} mice (4,18). In contrast, IGF-1R^{aP2Cre} mice have increased somatic growth, further suggesting that tissues other than fat and brain are not affected by the ectopic aP2-Cre transgene expression. However, we have to discuss our data with the caution that reduced IGF-1R expression in the brain may contribute to the phenotype of IGF-1R^{aP2Cre} mice. IGF-1R^{aP2Cre} mice are viable and fertile and do not exhibit growth retardation.

We demonstrate that IGF-1R^{aP2Cre} mice have increased somatic growth starting at an age of 10 weeks. IGF-1R^{aP2Cre} mice are both longer and heavier than their wild-type littermates. The increased growth is not the result of increased food intake in IGF-1R^{aP2Cre} mice.

Interestingly, adipose tissue, liver, and heart exhibit higher relative organ weights than other organs, including kidney, skeletal muscle, and spleen, which are increased in size proportionally to the higher body weight of IGF-1R^{ap2Cre} mice. Increased growth in IGF-1R^{ap2Cre} mice is most likely the result of an ~20% increased IGF-1 serum concentrations. In patients with acromegaly, elevated circulating IGF-1 levels cause increased adult growth and, at least in some patients, may lead to enlarged organs, including hepatomegaly (19) and acromegalic cardiomyopathy (20). In analogy to the phenotype of IGF-1R^{ap2Cre} mice, transgenic expression of human IGF-1 in mice causes a similar phenotype with 1.3-fold increased weight as a result of selective organomegaly without an apparent increase in skeletal growth (21). Moreover, liver-specific IGF-1 overexpression causes 50% increased serum IGF-1 levels and enhanced somatic growth (22).

Because circulating GH and IGF-2 levels are normal, increased IGF-1 serum levels in IGF-1R^{ap2Cre} mice are most likely the result of increased IGF-1 expression both in adipose tissue and liver and not of changes caused by an IGF-1R deficiency in the central nervous system. It is difficult to dissect whether adipose or liver-derived IGF-1 primarily increases circulating IGF-1 levels. Interestingly, we identified a negative feedback mechanism for IGF-1 mRNA expression in adipose tissue. In wild-type adipocytes, IGF-1 suppressed its own mRNA expression *ex vivo*, whereas this negative feedback was blunted in adipocytes isolated from IGF-1R^{ap2Cre} mice. However, increased IGF-1 expression in liver is more difficult to explain.

It is difficult to dissect whether adipose or liver-derived IGF-1 primarily increases circulating IGF-1 levels. Our experimental design does not allow for the distinction between hepatic or adipose tissue-derived IGF-1. It has been shown that IGF-1 and IGF-1R mRNA levels are differentially regulated in different tissues (23). Interestingly, presumably adipose tissue-derived IGF-1 does not inhibit hepatic IGF-1 expression as it was shown in the liver of GH-deficient dwarf rats after IGF-1 treatment (24). Another potential explanation for the absence of a negative feedback of IGF-1 on its own expression in liver might be that hepatocytes only express the IGF-1R in very little amounts (25). Alternatively, circulating IGF-1 could be modulated indirectly by affecting its binding proteins. Increased IGFBP-3 mRNA expression in liver in response to increased circulating IGF-1 from adipose tissue could be a potential mediator. Increase in IGFBP-3 was the best and independent predictor of increased IGF-1 serum concentrations in our IGF-1R^{ap2Cre} mice (27).

Moreover, deletion of the *IGF-1* gene in liver demonstrated that liver-derived IGF-1 is not crucial for somatic growth (26), suggesting that increased somatic growth in IGF-1R^{ap2Cre} mice is primarily due to increased adipose tissue expression. However, previous data suggest that systemic IGF-1 can feedback on hepatic IGF-1 mRNA expression in the GH-deficient state. Our IGF-1R^{ap2Cre} mice have normal GH serum concentrations (Table 1), suggesting that under normal GH levels, hepatic IGF-1 expression does not depend on the same feedback mechanism. Moreover, we cannot explain why increased IGF-1 levels did not cause decreased GH serum concentrations. Therefore, we cannot exclude that reduction of IGF-1R receptor signaling in individual tissues causes a disruption of physiological feedback mechanisms in other systems or tissues. Adipose tissue-derived signals other than circulating IGF-1, GH, and/or IGF-2 might cause increased

circulating IGF-1 levels and increased IGF-1 expression in liver and adipose tissue. Further studies are necessary to characterize these signals.

Circulating IGF-1 was shown to reduce IGF-1 mRNA expression in liver, whereas GH increases IGF-1 gene expression (23). In our model with normal GH but increased IGF-1 serum concentrations, one would expect decreased rather than the observed increased hepatic IGF-1 mRNA expression. One hypothesis is that lack of IGF-1R signaling in adipose tissue generates signals that indirectly increase both adipose and hepatic IGF-1 expression. However, GH and IGF-2 receptor expressions were indistinguishable between IGF-1R^{ap2Cre} and control mice in both liver and adipose tissue, suggesting that no liver-specific compensatory mechanism accounts for the unsuppressed IGF-1 mRNA expression in liver. In parallel to increased IGF-1 serum concentrations, circulating IGFBP-3, but not IGFBP-1 and -2, was significantly increased in IGF-1R^{ap2Cre} mice. Overexpression of human IGFBP-3 in transgenic mice results in selective organomegaly, including liver and heart (24), suggesting that increased IGFBP-3 levels contribute to organomegaly in IGF-1R^{ap2Cre} mice.

Increased circulating IGF-1 by 50% was shown to improve glucose tolerance in mice with a liver-specific overexpression of the *Igf-1* gene (22). Interestingly, we did not observe any improvement of glucose tolerance and insulin sensitivity in IGF-1R^{ap2Cre} mice, suggesting that 20% increased IGF-1 levels are not sufficient to enhance whole-body insulin sensitivity. IGF-1R^{ap2Cre} mice do not exhibit significant metabolic alterations. Interestingly, at the age of 12 weeks, when growth curves diverge, fasting blood glucose concentrations are significantly higher in IGF-1R^{ap2Cre} than in controls. Because glucose tolerance is normal at this age, it is difficult to establish causality for elevated glucose concentrations. Higher adipose tissue mass could contribute to these metabolic alterations. We also found lower adiponectin serum concentrations in IGF-1R^{ap2Cre} mice of both sexes. Lower circulating adiponectin levels further suggest that metabolic alterations in IGF-1R^{ap2Cre} mice at 12 weeks of age are a consequence of increased fat mass. Serum adiponectin negatively correlates with fat mass in mice (16) and men (28). Insulin and IGF-1 are capable of binding to each other's receptor, although with different affinities (29). Mice with a targeted disruption of the insulin receptor in adipose tissue (FIRKO mice) are protected from obesity and its metabolic alterations (16). Moreover, these mice exhibit specific morphological changes in adipose tissue, which could be due to a defect in adipose tissue development. We therefore expected alterations in adipose tissue of IGF-1R^{ap2Cre}, because IGF-1R was shown to be important in the growth and differentiation of adipocytes *in vitro* (9). Despite similarities in the structure and intracellular signaling between insulin and IGF-1Rs, we did not find a severe metabolic phenotype in mice lacking the IGF-1R in adipose tissue. However, we found significantly increased insulin-stimulated glucose uptake into isolated adipocytes from IGF-1R^{ap2Cre} mice, suggesting increased glucose uptake and subsequent increase in lipogenesis as primary causes leading to increased lipid load per adipocyte and adipose tissue hypertrophy in IGF-1R^{ap2Cre} mice.

This further suggests that insulin receptor signaling is more important for fuel metabolism, whereas IGF-1R mediates growth, and that one receptor cannot functionally compensate for the other receptor's absence (13).

Our data further show that IGF-1R signaling in adipocytes is not crucial for the growth, development, or differentiation of adipose tissue *in vivo*. Unexpectedly, both the number and the size of adipocytes is increased in adipose tissue of IGF-1R^{ap2Cre} mice, either suggesting that intact IGF-1R is not necessary for adipose tissue development or that other mechanisms exist *in vivo*, which can compensate for the disruption of IGF-1R. In accordance with our results, it was recently shown that most IGF receptor-deficient adipocyte cell lines were capable of normal differentiation (13). Moreover, important markers of adipogenesis, including peroxisome proliferator-activated receptor- γ and GLUT4, were expressed despite the lack of IGF-1R (13). One potential mechanism could be that insulin receptor mediates the IGF-1 effects on growth and differentiation *in vivo*. This hypothesis is supported by increased *insulin receptor* gene expression in adipose tissue of IGF-1R^{ap2Cre} mice. However, *in vitro* there was no compensation of insulin receptor when the IGF-1R was absent. Therefore, it appears that IGF-1R is not crucial for adipose tissue development. Interestingly, adipocytes from IGF-1R^{ap2Cre} mice were more sensitive to insulin-stimulated glucose uptake than adipocytes from control mice. Our findings are in accordance with previously reported increased insulin sensitivity in IGF-1R-deficient brown adipocytes (30). Moreover, downregulation of IGF-1R in breast cancer cells was shown to increase insulin sensitivity (31). Diminished IGF-1R/insulin receptor hybrid receptor formation resulting in enhanced homo-insulin receptor formation could contribute to increased insulin sensitivity in IGF-1R-deficient adipocytes. In addition, increased insulin receptor number might enhance insulin effects on IGF-1R^{ap2Cre} adipocytes.

In conclusion, IGF-1R signaling in adipocytes is not crucial for the development and differentiation of adipose tissue *in vivo* but seems to participate in the regulation of IGF-1 serum concentration.

ACKNOWLEDGMENTS

M.B. has received Deutsche Forschungsgemeinschaft Grant BL 580/3-1, Clinical Research group Atherobesity KFO 152 Project BL 833/1-1, and Project B24 from the Interdisciplinary Center of Clinical Research Leipzig at the Faculty of Medicine of the University of Leipzig.

REFERENCES

1. Dupont J, Holzenberger M: Biology of insulin-like growth factors in development. *Birth Defects Res* 69:257–271, 2003
2. Accili D, Drago J, Lee EJ, Johnson MD, Cool MH, Salvatore P, Asico LD, Jose LA, Taylor SI, Westphal H: Early neonatal death in mice homozygous for a null allele of the insulin receptor gene. *Nat Genet* 12:106–109, 1996
3. Liu JP, Baker J, Perkins A, Robertson EJ, Efstratiadis A: Mice carrying null mutations of the genes encoding insulin-like growth factor I (IGF-I) and type 1 IGF receptor (Igf1r). *Cell* 75:59–72, 1993
4. Holzenberger M, Dupont J, Ducos B, Leneuve P, Geloan A, Even PC, Cervera P, Le Bouc Y: IGF-1 receptor regulates lifespan and resistance to oxidative stress in mice. *Nature* 421:182–187, 2003
5. Zhang M, Xuan S, Boussein ML, von Stechow D, Akeno N, Faugere MC, Malluche H, Zhao G, Rosen CJ, Efstratiadis A, Clemens TL: Osteoblast-specific knockout of the insulin-like growth factor (IGF) receptor gene reveals an essential role of IGF signaling in bone matrix mineralization. *J Biol Chem* 277:44005–44012, 2002
6. Fernandez AM, Dupont J, Farrar RP, Lee S, Stannard B, Le Roith D: Muscle-specific inactivation of the IGF-I receptor induces compensatory hyperplasia in skeletal muscle. *J Clin Invest* 109:347–355, 2002
7. Coleman ME, DeMayo F, Yin KC, Lee HM, Geske R, Montgomery C, Schwartz RJ: Myogenic vector expression of insulin-like growth factor I stimulates muscle cell differentiation and myofiber hypertrophy in transgenic mice. *J Biol Chem* 270:12109–12116, 1995

8. Kulkarni RN, Holzenberger M, Shih DQ, Ozcan U, Stoffel M, Magnuson MA, Kahn CR: Beta-cell-specific deletion of the Igf1 receptor leads to hyperinsulinemia and glucose intolerance but does not alter beta-cell mass. *Nat Genet* 31:111–115, 2002
9. Smith PJ, Wise LS, Berkowitz R, Wan C, Rubin CS: Insulin-like growth factor-I is an essential regulator of the differentiation of 3T3-L1 adipocytes. *J Biol Chem* 263:9402–9408, 1988
10. Scavo LM, Karas M, Murray M, Le Roith D: Insulin-like growth factor-I stimulates both cell growth and lipogenesis during differentiation of human mesenchymal stem cells into adipocytes. *J Clin Endocrinol Metab* 89:3543–3553, 2004
11. Abel ED, Peroni OD, Kim JK, Kim YB, Boss O, Hadro E, Minnemann T, Shulman GI, Kahn BB: Adipose-selective targeting of the GLUT4 gene impairs insulin action in muscle and liver. *Nature* 409:729–733, 2001
12. Etherton TD, Thompson EH, Allen CE: Improved techniques for studies of adipocyte cellularity and metabolism. *J Lipid Res* 18:552–557, 1977
13. Entingh-Pearsall A, Kahn CR: Differential roles of the insulin and insulin-like growth factor-I (IGF-I) receptors in response to insulin and IGF-I. *J Biol Chem* 279:38016–38024, 2004
14. Ross SR, Graves RA, Greenstein A, Platt KA, Shyu HL, Mellovitz B, Spiegelman BM: A fat-specific enhancer is the primary determinant of gene expression for adipocyte P2 *in vivo*. *Proc Natl Acad Sci U S A* 87:9590–9594, 1990
15. Blüher M, Kahn BB, Kahn CR: Extended longevity in mice lacking the insulin receptor in adipose tissue. *Science* 299:572–574, 2003
16. Blüher M, Michael MD, Peroni OD, Ueki K, Carter N, Kahn BB, Kahn CR: Adipose tissue selective insulin receptor knockout protects against obesity and obesity-related glucose intolerance. *Dev Cell* 3:25–38, 2002
17. Urs S, Harrington A, Liaw L, Small D: Selective expression of an ap2/fatty acid binding protein 4-Cre transgene in non-adipogenic tissues during embryonic development. *Transgenic Res* 15:647–653, 2006
18. Holzenberger M, Leneuve P, Hamard G, Ducos B, Perin L, Binoux M, Le Bouc Y: A targeted partial inactivation of the Igf1r gene in mice causes a postnatal growth deficit. *Endocrinology* 141:2557–2566, 2000
19. Ezzat S: Hepatobiliary and gastrointestinal manifestations of acromegaly. *Dig Dis* 10:173–180, 1992
20. Colao A, Vitale G, Pivonello R, Ciccarella A, Di Somma C, Lombardi G: The heart: an end-organ of GH action. *Eur J Endocrinol* 151:S93–S101, 2004
21. Mathews LS, Hammer RE, Behringer RR, D’Ercole AJ, Bell GI, Brinster RL, Palmiter RD: Growth enhancement of transgenic mice expressing human insulin-like growth factor I. *Endocrinology* 123:2827–2833, 1988
22. Liao L, Dearth RK, Zhou S, Britton OL, Lee AV, Xu J: Liver-specific overexpression of the insulin-like growth factor-I enhances somatic growth and partially prevents the effects of growth hormone deficiency. *Endocrinology* 147:3877–3888, 2006
23. Lemmey AB, Glassford J, Flick-Smith HC, Holly JM, Pell JM: Differential regulation of tissue insulin-like growth factor-binding protein (IGFBP)-3, IGF-I and IGF type 1 receptor mRNA levels, and serum IGF-I and IGFBP concentrations by growth hormone and IGF-I. *J Endocrinol* 154:319–328, 1997
24. Butler AA, Ambler GR, Breier BH, LeRoith D, Roberts CT Jr, Gluckman PD: Growth hormone (GH) and insulin-like growth factor-I (IGF-I) treatment of the GH-deficient dwarf rat: differential effects on IGF-I transcription start site expression in hepatic and extrahepatic tissues and lack of effect on type I IGF receptor mRNA expression. *Mol Cell Endocrinol* 101:321–330, 1994
25. Butler AA, LeRoith D: Minireview: tissue-specific versus generalized gene targeting of the igf1 and igf1r genes and their roles in insulin-like growth factor physiology. *Endocrinology* 142:1685–1688, 2001
26. Yakar S, Liu JL, Stannard B, Butler A, Accili D, Sauer B, LeRoith D: Normal growth and development in the absence of hepatic insulin-like growth factor I. *Proc Natl Acad Sci U S A* 96:7324–7329, 1999
27. Murphy LJ, Molnar P, Lu X, Huang H: Expression of human insulin-like growth factor-binding protein-3 in transgenic mice. *J Mol Endocrinol* 15:293–303, 1995
28. Tschritter O, Fritsche A, Thamer C, Haap M, Shirkavand F, Rahe S, Staiger H, Maerker E, Haring H, Stumvoll M: Plasma adiponectin concentrations predict insulin sensitivity of both glucose and lipid metabolism. *Diabetes* 52:239–243, 2003
29. Steele-Perkins G, Turner J, Edman JC, Hari J, Pierce SB, Stover C, Rutter WJ, Roth RA: Expression and characterization of a functional human insulin-like growth factor I receptor. *J Biol Chem* 263:11486–11492, 1988
30. Mur C, Valverde AM, Kahn CR, Benito M: Increased insulin sensitivity in IGF-I receptor-deficient brown adipocytes. *Diabetes* 51:743–754, 2002
31. Zhang H, Pelzer AM, Kiang DT, Yee D: Down-regulation of type I insulin-like growth factor receptor increases sensitivity of breast cancer cells to insulin. *Cancer Res* 67:391–397, 2007